

# Revisiting the Carousel and Non-radial Oscillation Models for Pulsar B0809+74

Joanna Rankin<sup>1,2</sup> & Rachel Rosen<sup>3,4</sup>

<sup>1</sup>*Physics Department, University of Vermont, Burlington, VT 05405\**

<sup>2</sup>*Sterrenkundig Instituut ‘Anton Pannekoek’, University of Amsterdam, NL-1090 GE*

<sup>3</sup>*National Radio Astronomy Observatory, Charlottesville, VA 22091*

<sup>4</sup>*West Virginia University, White Hall, Morgantown, WV 26506†*

Accepted 2012 month day. Received 2012 month day; in original form 2012 month day

## ABSTRACT

Recent interest in pulsar B0809+74, well known for its highly accurate drifting subpulses and “memory across nulls” has raised questions about the adequacy of the rotating subbeam-carousel or/and non-radial oscillation models to describe this phenomenon. The success of the subbeam carousel model in explaining the drift modes and periodic nulls in B1918+19 (Rankin, Wright & Brown 2013) has encouraged us to revisit the application of this model to B0809+74. Pulsar B0809+74 is a complicated object, as are many pulsars where our sightline grazes the conal beam edge obliquely. Its subpulses also exhibit complex modal polarization, and only analyzing the total power paints an incomplete picture of emission from the star. This remarkable pulsar has, however, been studied in great detail for over three decades, and many of the earlier controversies about its characteristics have largely been resolved. In this paper, we demonstrate that the carousel model is highly successful in reproducing the behavior of B0809+74 in every heuristic and geometric manner. In addition, Rosen & Demorest (2011) have quantitatively fit a non-radial oscillation model to B0809+74 at a single frequency, and we address how this model can reproduce the behavior of B0809+74 across a much larger band.

**Key words:** – pulsars: general, individual (B0809+74)

## 1 INTRODUCTION

Radio pulsar B0809+74 is well known not only for its bright and precisely drifting subpulses but also for its exceedingly broad spectrum. It has been observed down to approximately 10 MHz and up to around 10 GHz, and unusually its spectrum hardly turns over at low frequency.

Remarkable new possibilities for acquiring high quality low frequency observations (*e.g.*, Hassell *et al.* 2013a,b; hereafter Hassall I/II) have revived interest in various aspects of this pulsar’s emission and subsequent interpretation. The phenomenology of B0809+74’s emission has proven to be quite complex, but most of the earlier controversies regarding its basic emission characteristics have by now largely been resolved. In particular:

### 1.1 Grazing sightline traverse

Every known well studied pulsar with broadly drifting subpulses has a sightline that just grazes the emission cone tangentially. This makes sense geometrically, and models of the basic emission geometry also bear it out. Such pulsars are denoted as conal single ( $\mathbf{S}_d$ ) or in some other cases as conal triple ( $\mathbf{cT}$ ) in the classification schema of the “Empirical Theory” (Rankin 1993; ETVI) and entail a ratio  $\beta/\rho$  of typically  $\sim |0.8|$  or more (where  $\beta$  is the sightline impact angle and  $\rho$  is the conal radius out to the outside half power point). Lyne & Manchester’s (1988; hereafter LM) work reaches very similar conclusions.

The conclusion that pulsars with well-organized drifting subpulses have a geometry where the sightline tangentially grazes the emission cone is also consistent with a non-radial oscillation model. Clemens & Rosen (2004) show, in Figure 3 of their paper, that the absence of a nodal line, such as in a conal geometry, leads to organized drifting subpulses. However, if a nodal line is

\* Joanna.Rankin@uvm.edu

† rachel.rosen@gmail.com

present, which would include some (but not all) double profiles, the nodal line modulates the subpulses and creates more complex behavior.

### 1.2 Incomplete profiles

In addition, most pulsars with grazing sightlines have profiles that are incomplete, or “absorbed”—often at meter wavelengths—that is, their widths are not as large as would be expected when extrapolating from lower frequency where the cone size is apparently larger and the emission extends roughly over the full angular width of the polar cap. Or, equivalently, that single-pulse correlation techniques show that an incomplete profile corresponds to only a part of a more complete one at some other frequency. It is not fully clear why this is so, but there are several obvious and probable reasons—

- the conal edge is not smooth or even jagged as in the Deutsch (1955) or other conal beam models
- because the sightline traverse is so shallow that it never penetrates as far as the radial peak and is thus incommensurate with the dimensions of lower frequency profiles where it does.
- the emission mechanism is itself asymmetric about the longitude of the magnetic axis for a host of possible reasons (intrinsic strength, degree of coherence, aberration/retardation, etc.)
- or perhaps because there is actual physical absorption (or scattering) above a part of the polar cap. Indeed, given the huge magnetic field and dense plasma in the inner magnetosphere, it is difficult to see how the absorption could be less than total!

Therefore, B0809+74 is typically and expectedly complex in this regard compared to other well studied pulsars with profiles reflecting grazing sightlines. And this complexity associated with incomplete profiles seems to occur primarily at meter or higher frequencies where the sightline traverses are often shallower than expected. Another well known drifter, B0943+10, shows time-variability in the completeness of its B-mode profile after onset (Rankin & Suleymanova 2006). Paper ET VI found that geometrical models could not be as precise for  $S_d$  stars because of the above. Mitra & Rankin (2010; ET IX) found that many of LM’s “partial cones” are in fact conal single pulsars with incomplete profiles stemming from grazing sightlines.

Incomplete profiles, aka “absorption” (note the quotes), are a matter of observable fact—and not uncommon among the normal pulsar population. Parts of B0809+74’s profiles are missing at certain frequencies, and yet we cannot yet be fully sure which profiles and frequencies are affected. Single-pulse correlations between certain bands show this clearly. For instance, when 380-MHz pulses are correlated against their 1400-MHz counterparts, we see that the drifting subpulses in the leading part of the latter have no counterparts in the former—whereas those in the trailing part of the profile do (*e.g.*, Rankin *et al.* 2006, hereafter Paper 1: fig. 4).

“Absorption” is thus not a theoretical interpretation, it is an observationally demonstrable effect. Bartel *et al.* (also Bartel) (1981) named it—perhaps poorly—and at

low frequencies in B0809+74 it produced the appearance of “superdispersion” (*e.g.*, Shitov & Malofeev 1985). While the physical process behind “absorption” is poorly understood, the observable effects are well documented.

### 1.3 Depolarized conal edges

The edges of conal beams corresponding roughly to the “last open field lines” of the polar flux tube are virtually always highly depolarized (Rankin & Ramachandran 2003; ET VII). This edge depolarization is an important characteristic of conal beams and appears to result from the circumstance that the two orthogonal polarization modes (OPMs) have comparable strengths on the outer edges of cones. In pulsars with regular subpulse modulation, this edge depolarization is produced by sets of primary- and secondary polarization mode (PPM and SPM) ‘beamlets’ or subpulses offset from each other by about 180° in modulation phase.

Conversely, such edge depolarization provides a reliable means of identifying the edges of cones. B0809+74’s high frequency profiles show no such edge depolarization on one or both wings of their profiles, whereas its lower frequency profiles show ever more. Indeed, the leading edges of the pulsar’s profiles at 1 GHz and above are nearly unique in exhibiting almost complete linear polarization; such high linear polarization is very rare in conal profiles and indicates that the sightline is encountering a single fully polarized OPM in this region.

### 1.4 Dynamic profile structure

The concept of a pulsar “component” is a bit fuzzy at best. However, in many cases it is the intensity-weighted distribution function of subpulses that accrue almost randomly within a restricted region of longitude. Therefore, we can talk meaningfully about the structures of pulsars with two, three or even five components whose widths are relatively narrow compared to the overall profile width.

However, conal single profiles are not like pulsars with multiple components. Rather, they aggregate the emission from individual subpulses that *systematically* drift through them. Various geometrical and physical factors contribute to the intensity level at different longitudes, so there will be little clear meaning to a peak or to some combination of constituent Gaussian forms.

### 1.5 Multifrequency profile alignment

The common method of aligning pulsar profiles across many frequencies is to use the known dispersion such that similar instants at different frequencies are placed on a common /bf basis—as if we were observing in the immediate vicinity of the pulsar. Conversely, short duration broadband effects can be used to determine the dispersion as did Bruk *et al.* (1986) for B0809+74 at low frequencies using microstructure.

Using dispersion alignment, conal profile centers align closely—as long as they are complete—for instance, as evidenced by their depolarized edges. B0809+74’s higher frequency incomplete profiles can then be aligned

only by dispersion—that is, similarly to those seen in Paper 1: fig. 3.

However, it is problematic on several grounds to use B0809+74’s profiles of themselves to establish a reliable alignment, because some of the profiles are incomplete. The proper methodology is to align not the profiles but the constituent subpulses and/or microstructure (to the extent possible given conal spreading at low frequency).

### 1.6 Basic emission geometry

Geometric models using both profile width and polarization provide reasonably accurate and consistent basic emission geometry—that is, the magnetic latitude  $\alpha$  and sightline impact angle  $\beta$ , though as for most pulsars it is difficult to determine whether  $\beta$  is positive (equatorward) or negative (poleward). Further, the Thorsett (1991) model provides a very adequate description of conal spreading at low frequency. For B0809+74,  $\alpha$  is about  $9^\circ$  and  $\beta \pm 5^\circ$  (see Paper 1: Tables 2/3).

### 1.7 Drifting subpulse “phase jumps”

Discontinuities in the modulation phase (“phase jumps”) of drifting subpulses near the centers of certain profiles are common. They can occur when either: a) incommensurate intervals of magnetic and rotational phase accrue between leading and trailing portions of a profile, or b) the two parts of the pulse profile (leading and trailing) have different OPMs. In these situations, a roughly  $180^\circ$  modulation-phase “jump” will occur at the boundary.

These effects are seen in a few different pulsars and the OPM-related “jumps” are readily understood within the carousel model when they are analyzed polarimetrically. Several examples of such effects are shown in Rankin *et al.* (2005), hereafter Paper 0: figs. 5/6; however, we now see that the graphical presentation was not completely clear. We give here revised versions of these modulation-folded displays in Figure ??, that show *both* the total power (contours) and modal polarization (colour scale) behaviour of the driftbands.

## 2 REVISITING B0809+74’S CAROUSEL MODEL

### 2.1 Dispersion Alignment

A rotating subbeam-carousel model for B0809+74 makes no physical sense unless we view each member ‘beamlet’ of such a system as potentially radiating over the entire radio-frequency spectrum. This in turn requires that the observations in each band be aligned, in principle, such that a polarized beamlet momentarily passing the central longitude (of the magnetic axis) be simultaneous—and note that the central longitude does not necessarily mean the center of the pulse profile, as discussed in §1.2. This is the dispersion alignment which was determined accurately and at very low frequency by Smirnova *et al.* (1986) to entail a dispersion measure of  $5.751 \pm 0.003$  pc/cm<sup>3</sup> [see also Bruk *et al.* (1986) and Popov *et al.* (1987)]. Various earlier analyses were made to determine

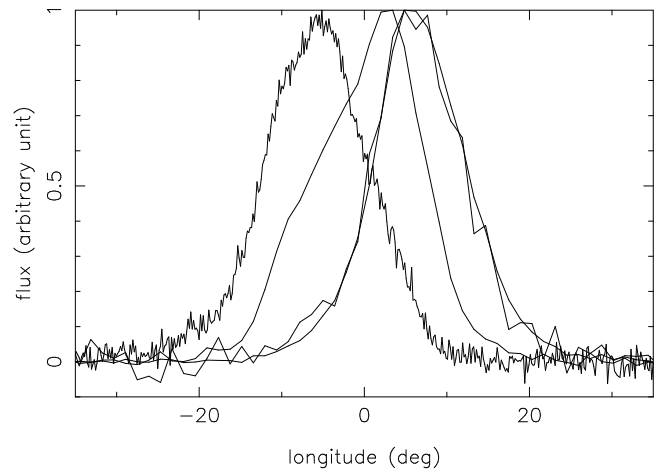


**Figure 1.** A display of profiles at 382 (rightmost profiles), 1375 (center profile) and 4880 MHz (lefthand profile) assembled to explore the high frequency alignment from Paper 1 (see this paper for details). Apparently, none of the pulsar’s profiles in the centimeter-wavelength region have edges that align in a simple manner.

how B0809+74’s high frequency emission aligned using single-pulse cross correlations. These efforts of course drew on observations far inferior to those now available (see Hassall I and II), but found the dispersion measure to be similar to that of these 25-year old observations. Furthermore, Bruk *et al.* (1986) and Popov *et al.* (1987) developed a robust, and still relevant, methodology of correlating measurements across multiple frequencies.

The Hassall I analysis presents a huge collection of observations and exhibits strongly the remarkable power and broad capabilities of the new LOFAR instrument. Their alignment of their multifrequency profiles, however, is based on a single Gaussian-fitted component across all frequencies. This alignment technique potentially suffers from all of the issues discussed in the foregoing section, and their analysis does not address the “absorption” and putative “superdispersion” encountered by earlier investigators.

This said, Hassall I appears to measure a compatible DM value of 5.75 pc/cm<sup>3</sup>—not, however, by a technique that can be directly compared with the older measurements above. Given B0809+74’s history and complexity, one or the other above microstructure techniques provides by far the most reliable method for aligning its profiles and subpulses. There are several issues, both with prior and current observations and analysis that need to be resolved. First, Bruk *et al.* do not clearly state that their value aligns the centers of their low frequency profiles.

Second, their measurements are now almost three decades old, and while most pulsar DM values are fairly stable in time, this should not be taken for granted. A new low frequency microstructure determination is now certainly warranted, and this might be carried out even

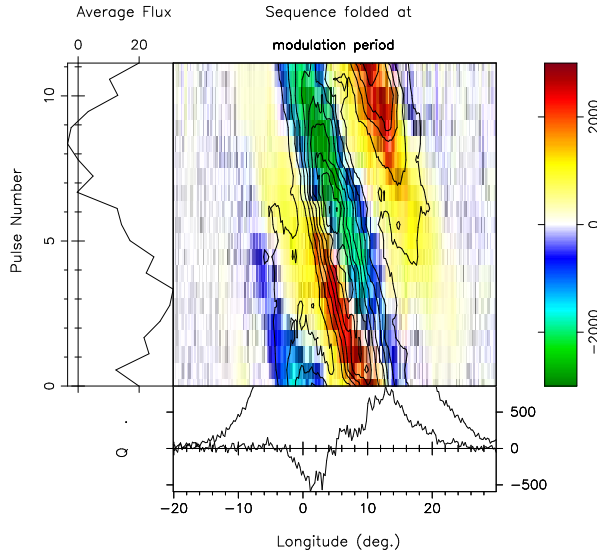


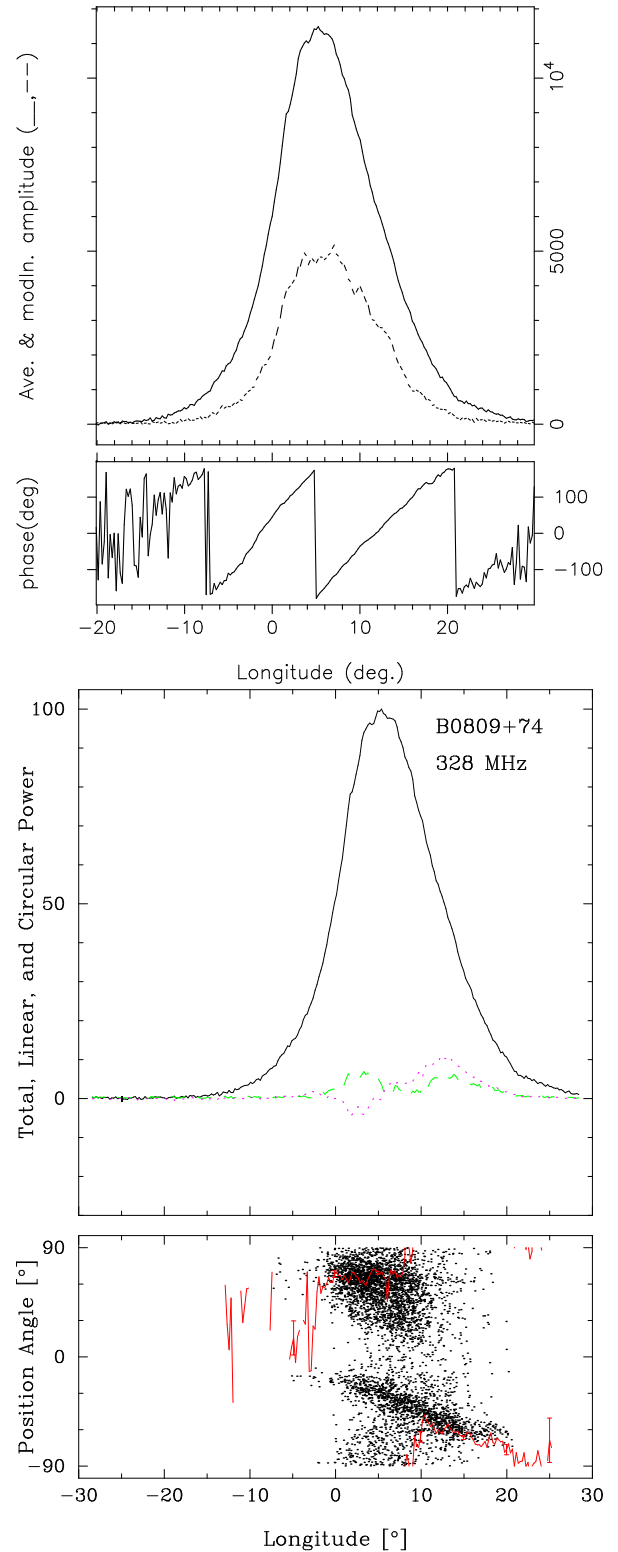
**Figure 2.** Folded 328-MHz driftband (top left) showing the total power (contours) and the modal polarization (colour-intensity coded) in terms of the rotated Stokes parameter  $Q'$  (see Paper 0 for details). The two OPMs are coded positive and negative, and close inspection shows that the total power driftband is canted with respect to the two modal overlapping driftbands. (top right) A display of the total power modulation phase, with the profile and the modulated power in the top panel and the phase in the lower one. (bottom right) Polarized profile of the same pulse sequence. The overall depolarization is striking, and one can see that the two regions of modal polarization overlap more in the leading region than the trailing.

with existing LOFAR observations.<sup>1</sup> The calculation of the DM from the microstructure might be possible from the data collected by Hassall *et al.* Third, if the Bruk *et al.* value remains correct, and if further it aligns the profiles as depicted in Hassall I: fig. 11, then it may be possible that the pulsar’s profile incompleteness is a serious consideration. It is even possible that B0809+74 is a conal triple (cT) configuration wherein the inner cone is visible as their aligned “component”, the trailing sightline traverse through the outer cone produces their trailing feature at lower frequencies, and the leading outer conal component is missing over the entire long wavelength region? Were this the case, it could explain much, very possibly including some of the “kinks” in the driftbands.

## 2.2 Driftband analysis

Much of the analysis in Hassall II is beautifully carried out according to the framework established in Hassall I. More than any other pulsar, it is difficult and risky to undertake an analysis of B0809+74 drifting subpulses on the sole basis of total power. Indeed, there is a bit of confusion in number of early papers (reviewed in Paper 0) because the analysis only considered the total power and did not take into account the polarization properties of the pulsar.

<sup>1</sup> The Hobbs *et al.* (2004) value of  $6.116 \pm 0.018$  from timing seems unreliable for the present purposes.



The polarized subbeam maps in Paper 2: fig. 4 demonstrate why a total power analysis is incomplete for B0809+74. Similar depictions can be found in Ramachandran *et al.* (2002) and Edwards (2004). In this pulsar at high frequency, the PPM and SPM beams have comparable power, whereas in other pulsars the PPM beamlets are more dominant. Note what is done here: the polar-

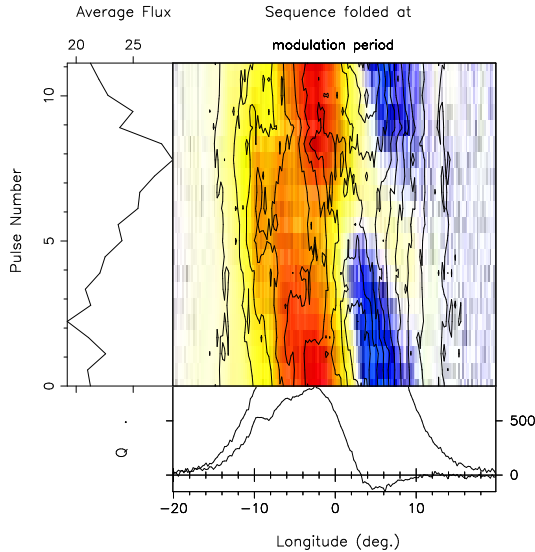
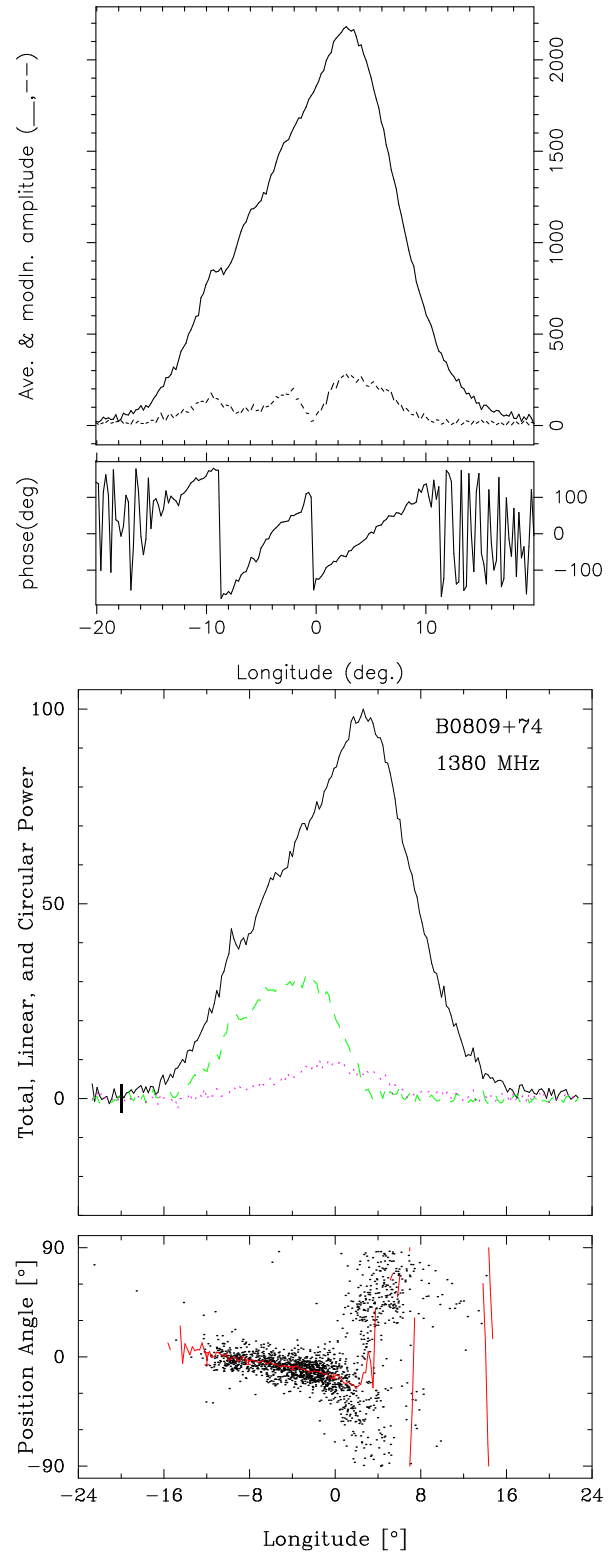


**Figure 3.** Folded 1380-MHz driftband (top left) showing the total power (contours) and the modal polarization (colour-intensity coded) in terms of the rotated Stokes parameter  $Q'$  (see Paper 0 for details). The two OPMs are coded positive and negative, and one can see that the driftband is comprised of two different OPMs and that they change sharply in the center of the profile. (top right) A display of the total power modulation phase, with the profile and the modulated power in the top panel and the phase in the lower one. Note the roughly  $180^\circ$  modulation phase change at  $0^\circ$  longitude associated with the OPM transition. (bottom right) Polarized profile of the same pulse sequence. The contrasting large fractional linear polarization in the leading part of the profile and complete depolarization in the latter half is striking.

ized power is rotated into a single Stokes parameter  $Q'$  so that PPM power is shown positive and SPM negative. These 10-beam maps show that the sightline cannot help but encounter both sets of OPM beamlets, generating a complex admixture that conflates, depolarizes and alters the timing of their resulting combination.<sup>2</sup>

The argument in Hassall II is correct that there are two sets of overlapping drift bands at high frequency. But when one compares the corresponding panels of their fig. 5 with the polarized folded driftbands of Paper 0: figs. 5/6, it appears that these two driftbands correspond to the two OPMs. At 1380 MHz one OPM is active in the early part of the profile over the entire modulation cycle, whereas both compete in the trailing region over portions of the cycle to depolarize the profile. Then, at 328 MHz we see that the two OPMs more nearly overlap throughout the modulation cycle.

A problem with this analysis in Paper 0 is that the total power driftband was not shown, so a reader could not see as clearly as needed how it is that the total power and polarized driftbands behave differently. We have repaired that in Figures 2 and 3 here. At 328-MHz the



Stokes  $I$  driftband is somewhat canted with respect to the modal driftbands, but there is no discontinuity in modulation phase, and two OPM driftbands almost completely depolarize the overall profile. At 1380-MHz the situation is very different: one OPM is associated with the driftband in the early part of the profile and another in the trailing half with a sharp transition midway. This results

<sup>2</sup> Hassell I makes one polarization argument in their fig. 13, and what is impressive about this figure is the broadband character of the *depolarization*, such that little sense can be made out of the residuum.

in the roughly  $180^\circ$  modulation-phase step identified by many writers. Here, very unusually, the leading part of the profile is highly linearly polarized and the trailing part highly depolarized.

What happens at lower frequencies is perhaps less of a polarization effect, but even at around 100 MHz we can see in Paper 0: fig. 3 that the two OPMs are overlapping but such that one is much stronger in the leading and the other in the trailing portions of the profile. At decameter wavelengths the driftbands further divide not because of polarization but because here the star's profile begins to have actual component structure due to conal spreading—dividing progressively into an apparent conal double configuration.

### 2.3 “Frequency Dependent Delay”

The depiction of B0809+74's driftbands in Hassall II: fig. 5 is very impressive in terms both of quality and extent, especially into decameter wavelengths. However, their interpretation leading to a putative “frequency dependent delay”, stemming from the great length of the driftbands at low frequency, is flawed and incorrect.

Most use of the rotating carousel-beam model is still unfortunately more geometry than physics—all due respect to Ruderman & Sutherland (1975) notwithstanding. Nonetheless, if one wishes to assess the efficacy of this model, the analysis must be conducted in the context of a full geometrical model of the carousel-beam emission of the pulsar, which Hassall II did not attempt.

The carousel model expects more driftbands at low frequency compared to high frequency and that the driftbands become longer across pulse longitude, and this trend is observed in B0809+74. Hassall II: fig. 5 shows that hardly two (or at most three) driftbands occupy the width of the profile at any frequency down to 100 MHz—and that these driftbands persist for times hardly longer than the 11-rotation-period  $P_3$ . At decameter wavelengths, however, the number rapidly increases to some 5 at perhaps hardly an octave lower; and the bands persist for 3 or even most of 4 times  $P_3$ .

This behavior is completely expected within the carousel model. For the same reason that the profile bifurcates into first two unresolved components and ultimately two well resolved ones—indicating that the sightline traverse is ever more central—the overall width of the profile spans more beamlets. Moreover, because these beamlets are regularly spaced in magnetic azimuth, the (rotationally centered) sightline arc between the edges of the profile becomes progressively shorter than the magnetic azimuth arc. This has the effect of crowding beamlets (or driftbands) into the growing width of the profiles at decameter wavelengths.

For instance, in the 32-MHz panel, it takes a very long time for a particular beamlet (or subbeam) to rotate across the full width of the profile—indeed, something upwards of 40 stellar rotations. Therefore, Hassall II's “frequency dependent delay” actually entails rather little physical delay. Rather, it is primarily the expected rotational phase delay. Because their analysis did not include the geometry and dynamics of the rotating carousel, they

interpreted what is mostly a rotational phase delay as a physical time delay.

Therefore, there the subbeam-carousel model of pulsar B0809+74's drifting subpulses remains an accurate description of the complex behavior that this pulsar exhibits. Indeed, the characteristics of this carousel beam system can be modeled quantitatively in some detail as was done in Paper 2: Tables 2/3. Note in particular that  $P_2$  is virtually constant down to 100 MHz and further increases slowly down to 17 MHz—and it is interesting to compare these values with the overall profile widths. Clearly, the long wavelength profile widths grow very much faster than  $P_2$ . Note that this is true irrespective of how the high frequency profile widths are modeled.

### 3 REVISITING B0809+74'S NON-RADIAL OSCILLATION MODEL

In a series of papers, Clemens & Rosen developed a non-radial oscillation model to describe drifting subpulses and their associated behavior. The fundamental assumption of the model is that the neutron star is undergoing non-radial oscillations of high spherical degree ( $\ell$ ) aligned with the magnetic axis which modulate the radio emission in addition to the rotational modulation. The average pulse shape and number of components are determined by the number of latitudinal nodes contained in the polar cap. The standing wave oscillations modulate the radio emission at a frequency (in general) incommensurate with the spin period of the pulsar. The modulated emission is manifested in the form of drifting subpulses or quasi-stationary behavior, where the amplitudes of the individual pulses in each component are modulated in a cyclic fashion.

Clemens & Rosen (2004) only addressed the total power observations of pulsars and modeled it accordingly. Clemens & Rosen (2008) expanded the model to include polarization behavior, specifically the two polarization modes. This included a scalar parameter, quantitatively fit by the model to the data, that relates the intensity of the two polarization modes. The model did not address multi-wavelength observations and, by default, assumed that the ratio of the strength of the two modes in the model was constant with observational frequency.

The three objections to a non-radial oscillation model discussed in Hassell II are reasonable when considering only the total power and given the limited scope of the model at a single frequency.

First, Hassell II re-states that a requirement of a non-radial oscillation model is that the nodal lines should intrude subpulse phase steps of exactly  $180^\circ$  as cited in Clemens & Rosen (2004). This is accurate when only considering the total power and only a single polarization mode. As shown in Figure 4 of Clemens & Rosen (2008), the ratio of the intensity of the two polarization modes can create subpulse phase jumps that are not equal to  $180^\circ$ . In Rosen & Demorest (2011), the fit of the non-radial oscillation model to the data produced a phase jump greater than  $180^\circ$  due the ratio of the two polarization modes. (The fact that fitting the model to the data resulted in a simulated phase jump of  $187.7^\circ$  phase

jump rather than a  $145.1^\circ$  phase jump is because the model fits the Stokes parameters directly and the phase jump indirectly.) If we assume, in the model, that both the ratio of the two polarization modes and the sightline is constant with observational frequency, Hassell II is correct in their assumption that it is unlikely that the subpulse phase step would increase systematically with observational frequency. Yet, as shown in Figures 3 and 2, the ratio of the polarization modes does change with frequency. The combination of a change in sightline traverse with observational frequency [see Discussion in Rosen & Demorest (2011) and the Introduction of this paper] and the change in the ratio of the two polarization modes with observational frequency could produce a systematic change in subpulse phase.

From a theoretical standpoint, if we assume that the oscillations occur on the stellar surface, their polarization characteristics should be independent of observational frequency. However, any surface motion would be tied to the magnetosphere in a way that is not well-understood; it is conceivable that modeling the multi-frequency observations with variable amplitudes for the polarization modes does *not* rule out surface oscillations.

Secondly, Hassall II points out that a requirement of the non-radial oscillation model is that the spacing of the components should follow the distribution of a spherical harmonic sampled along the line of sight. This requirement of the model was clearly stated in Clemens & Rosen (2004), and it was assumed that the center of the spherical harmonic aligned with the center of the pulse profile. Hassall II correctly notes that the size of the components in B0809+74 is equal, thus violating a requirement of the non-radial oscillation model. As the model was adapted to incorporate polarization in Clemens & Rosen (2008), it also included a “pulse window” that is separate from the pulsation model and limits the effects of the pulsations to the regions where emission occurs (Rosen & Clemens 2008). The non-radial oscillation model initially used a Gaussian to simulate the pulse window (Rosen & Clemens 2008) but was later adapted to use the average of the pulse profile (Rosen & Demorest 2011). The addition of the pulse window can cause both the spacing and the width of the pulse components to deviate from a spherical harmonic. Furthermore, as discussed in the Introduction, B0809+74 possibly has an incomplete profile, which would mean that the spherical harmonic does not align with the center of the pulse profile.

Finally, Hassall II notes that the non-radial oscillation model cannot explain how the subpulse phase begins on the leading edge of the pulse profile at low frequencies and moves through to the trailing edge at high frequencies. This is only true if the change in sightline with observational frequency is not considered. As the observational frequency changes, the sightline samples closer or further from the magnetic pole (Smits 2006) depending on the geometry. As the sightline traverse nears the magnetic pole, the nodal regions become smaller, effectively moving the nodal lines in longitude. Assuming a conal geometry and a potentially incomplete pulse profile, the nodal line (and thus subpulse phase jump) could systematically change with longitude.

## 4 DISCUSSION

### 4.1 The B0809+74 Carousel Model

Extensive efforts were made in the preparation of Papers 1/2 to determine the carousel geometry and circulation time (hereafter CT) of pulsar B0809+74. Any interpretation of the emission geometry, of course, is complicated by the various incomplete (or “absorbed”) high frequency profiles. Indeed, the 1400-MHz profile appears to be most complete (relative to higher and lower frequencies) but it is obviously not complete because it shows no edge depolarization—especially on its highly linearly polarized leading edge, making it difficult to assess the completeness of the profile. Therefore, Paper 1 gives two geometric models that made a “narrow” and “broad” assumption about how much of the profile is missing at 1380 MHz. What then is clear is that these bracketing models do not differ much in their values for  $\alpha$  and  $\beta$ , half a degree for the former and hardly  $0.2^\circ$  for the latter. Therefore, it can hardly be doubted that the magnetic latitude  $\alpha$  is about  $8-9^\circ$  and the impact angle  $\beta$  some  $4.5-5^\circ$  for B0809+74.

With regard to determining the carousel CT, we were perhaps less successful. At first we expected the drift-modulation frequency to be highly aliased because extrapolation from B0943+10’s value (Deshpande & Rankin 1999, 2001; hereafter DR) suggested that it could be as short as  $6.4 P_1$ . Moreover, B0809+74 does null as was so famously studied by Lyne & Ashworth (1983)—and on the basis of the pulsar’s “memory across nulls” we sought evidence of the CT in artificial null-removed sequences. The pulsar’s fluctuation spectra are of remarkably high quality and appeared more coherent when the nulls were removed. Disappointingly, though, they were devoid of features other than that of the primary modulation and a weak harmonic. Therefore, we never found indication of any CT in this manner or in more sophisticated inverse-cartographic mapping searches.

Some relief came from the pulsar’s nulls, by which van Leeuwen *et al.* (2002, 2003) in two important papers showed that the carousel recovery after nulls indicated that the primary fluctuation frequency was not aliased—and therefore was of alias order 0. But while this implied that the CT is merely some subbeam multiple of the drift band separation  $P_3$ , it in turn raised the specter that the CT might be very long, several hundreds of rotation periods. Using the various means described in Papers 1/2, we tested this possibility, and the results were that the pulsar probably has some 9/11 beams if an outside sightline traverse and roughly 25-40 if an inside traverse. This then implied that the CT could be in the range 75-90 secs in the first case and 6-9.5 mins in the latter one. Subbeam maps corresponding to these two possible situations, a 34-beam and a 10-beam (polarized) one for the two cases, respectively, are given in Paper II: figs. 3/4. With 20-20 hindsight we have wondered if an error was made in searching for carousel “solutions” using the null-removed sequences; however, we also relied heavily on a natural sequence of length 858 pulses that was null free.

#### 4.2 Status of the Carousel Model

The carousel model in more or less the form first articulated by Ruderman & Sutherland (RS) has proven highly successful, first in understanding the structure of B0943+10's system (DR) and then the normal 11- $P_1$  drift of B0809+74. In the interval further studies have strongly suggested that carousel action drives conal phenomena in many or even most pulsars (Weltevrede *et al.* 2006, 2007). Null related phenomena have provided further indications regarding CTs, in a few cases very reliably (*e.g.*, Rankin & Wright 2008; Herfindal & Rankin 2007, 2009)—and we have learned how complex nulling together with fluctuation-spectral evidence can be in, for instance, the recent work on B1918+19 (RWB)—so overall the carousel model does seem to provide both quantitative description and qualitative understanding of several related and interacting complex processes.

More to the point here, however, is to state clearly that the carousel model is yet an heuristic model that provides frustratingly little physical insight. All the measured CTs are well longer than envisioned by RS, and the partially screened revisions by (Gil *et al.* 2003, 2008) may provide better guidance or perhaps the recent work by Timokhin & van Leeuwen (2012). The model gives little understanding about the number and spacing of the sub-beam's parent "sparks". It provides no guidance whatsoever in understanding why the two concentric cones in double cone pulsars have phase-locked sets of drifting subpulses. It gives no explanation for why the displaced sets of modal subbeams on outer conal edges are usually displaced in magnetic longitude by half their angular separation. Finally, it provides no way to understand why only some of the rotating 'beamlets' are visible along our sightline (and in B0943+10 a varying number after B-mode onset) giving clear credence to the incomplete profile phenomenon (but not illuminating the physics) of this "absorption". Finally, returning specifically to B0809+74, the carousel model gives no insight into this pulsar's unique "memory across nulls" phenomenon.

#### 4.3 Status of the B0809+74 Non-radial Oscillation Model

The non-radial oscillation model was first developed in Clemens & Rosen (2004, 2008) and applied to pulsar B0943+10 in Rosen & Clemens (2008). Pulsar B0809+74, despite its often precise drifting, shows more complex behavior than B0943+10 in almost every way: polarization, profile evolutions, phase behavior, etc. Rosen & Demorest (2011) applied the non-radial oscillation model to B0809+74 at a single frequency.

Hassall II conducted a multi-frequency analysis of B0809+74 and discussed some difficulties that the non-radial oscillation model has in explaining the complex behavior. We address these difficulties, specifically the original total power formulation of the model exhibited difficulties that were repaired in the later papers, but their ramifications were not explicitly stated. Further, we discuss possible ways the model can be adapted for multiple frequency observation.

As this discussion demonstrates, more detailed test-

ing of the non-radial oscillation model in the B0809+74 context proves difficult and inconclusive for many of the same reasons that frustrated assessment of the carousel model: we simply do not yet have an adequately clear model of its profile evolution and emission geometry. Both models require estimates of the magnetic axis longitude, something that the Hassall papers did not attempt, and without it little further can be determined.

Nonetheless, the non-radial oscillation model retains great appeal. It is founded on a phenomenon well known for white dwarfs and thus utterly plausible for neutron stars. Many questions remain about the excitation and driving mechanism for oscillations in neutron stars. However, by showing that a phenomenological model for oscillations in neutron stars can quantitatively reproduce the observed behavior, we can then use our findings (such as oscillation frequency as a function of spherical degree) to assist in the development of the theoretical framework for both oscillations and how the oscillations are coupled to the emission process.

In summary, the relative successes of the carousel model have thrown its lack of any strong physical foundation into even clearer focus. Similarly, major uncertainties still remain between the appealing physical foundations of the non-radial oscillation model and its practical application. Perhaps the two approaches might support some hybrid physical model.

**Acknowledgments:** Portions of this work were carried out with support from US National Science Foundation Grants AST 08-07691. This work used NASA ADS system.

#### REFERENCES

- Barnard, J. J. & Arons, J. 1986, *Ap.J.*, 302, 138
- Bartel, N., Kardeshev, N. S., Kuzmin, A. D., Nikolaev, N.Ya., Popov, M.V., Sieber, W., Smirnova, T.V., Soglasnov, V.A., & Wielebinski, R. 1981, *A&A*, 93, 85.
- Bartel, N. 1981, *A&A*, 97, 384.
- Bruk, Yu. M., Ustimenko, B. Yu., Popov, M. V., Soglasnov, V. A., & Novikov, A. Yu. 1986, *Sov. Astron. Lett.*, 12, 381.
- Clemens, J. C., & Rosen, R. 2004, *Ap.J.*, 609, 340
- Clemens, J. C., & Rosen, R. 2008, *Ap.J.*, 680, 664
- Blaskiewicz, M., Cordes, J.M., & Wassermann, I. 1991 *Ap.J.*, 370 643.
- Deshpande, A. A., & Rankin, J. M. 1999, *Ap.J.*, 524, 1008
- Deshpande, A. A., & Rankin, J. M. 2001, *MNRAS*, 322, 438 (DR)
- Deutsch, A. J. 1955, *Ann. Astrophys.*, 18, 1
- Edwards, R. T. 2004, *A&A*, 426, 677
- Gil, J., Melikidze, G. I., & Geppert, U. 2003, *A&A*, 407, 315
- Gil, J., Haberl, F., Melikidze, G. I., Geppert, U., Zhang, B., & Melikidze, G. Jr. 2008, *Ap.J.*, 686, 497
- Hassall, T. E., Stappers, B. W., Hessels, J.W.T., Kramer, M., ++ 2012, *A&A*, 543, A66 (Hassall I)
- Hassall, T. E., Stappers, B. W., Weltevrede, P., Hessels, J.W.T., ++ 2012, *A&A*, in press (Hassall II)



- Hassall, T. E., 2013, private communication
- Herfindal, J. L., Rankin, J. M. 2007, *MNRAS*, 380, 430
- Herfindal, J. L., Rankin, J. M. 2009, *MNRAS*, 393, 1391
- Hobbs, G., Lyne, A. G., Kramer, M., Martin, C. E., & Jordan, C. A. 2004, *MNRAS*, 353, 1311
- Lyne, A.G., & Ashworth, M. 1983, *M.N.R.A.S.*, 204, 519
- Lyne, A.G., & Manchester, R.N. 1988, *M.N.R.A.S.*, 234, 477 (LM88)
- Mitra, D., & Rankin, J. M. 2011, *Ap.J.*, 727, 92 (ET IX)
- Rankin, J. M. 1993, *Ap.J.*, 405, 285 and A&A Suppl., 85, 145 (ETVI)
- Popov, M. V., Smirnova, T. E., & Soglasnov, V. A. 1987, *Soviet Astronomy*, 31, 529
- Ramachandran, R., Rankin, J.M., Stappers, B. W. Kouwenhoven, M.L.A., and van Leeuwen, A.G.L 2002, *A&A*, 381, 993
- Rankin, J.M., Ramachandran, R. 2003, *Ap.J.*, 590, 411 (ET VII)
- Rankin, J.M., Ramachandran, R., & Suleymanova, S. A. 2005, *A&A*, 429, 999 (Paper 0)
- Rankin, J.M., Ramachandran, R., & Suleymanova, S. A. 2006, *A&A*, 447, 235 (Paper 1)
- Rankin, J.M., Ramachandran, R., van Leeuwen, J., & Suleymanova, S. A. 2006, *A&A*, 455, 215 (Paper 2)
- Rankin J. M., & Suleymanova, S. A. 2006, *A&A*, 453, 679 (Paper IV)
- Rankin J. M., & Wright, G.A.E. 2008, *MNRAS*, 385, 1923
- Rankin J. M., Wright, G.A.E., & Brown, A. M. 2013, *MNRAS*, in press (RWB)
- Rosen, R., & Clemens, J. C. 2008, *Ap.J.*, 680, 671
- Rosen, R., & Demorest, P. 2011, *Ap.J.*, 728, 156
- Shitov, Yu.P., & Malofeev, V.M. 1985, *Sov. Astr. Lett.*, 11, 39.
- Ruderman, M., & Sutherland, P. 1975, *Ap.J.*, 196, 51
- Smirnova, T. V., Soglasnov, V. A., Popov, M. V., & Novikov, A. Yu. 1986, *Soviet Astronomy*, 30, 51
- Thorsett, S.E. 1991, *Ap.J.*, 377, 263.
- van Leeuwen, J., Kouwenhoven, M.L.A, Ramachandran, R., Rankin, J.M., & Stappers, B. W. 2002, *A&A*, 387, 169
- van Leeuwen, J., Ramachandran, R., Rankin, J.M., & Stappers, B. W. 2003, *A&A*, 399, 223
- van Leeuwen, J., & Timokhin, A. N. 2012, *Ap.J.*, 752, 155
- Weltevrede, P., Stappers, B. W., van den Horn, L. J., & Edwards, R. T. 2003, *A&A*, 412, 473
- Weltevrede, P., Edwards, R. T., & Stappers, B. W. 2006, *A&A*, 445, 243.
- Weltevrede, P., Stappers, B. W., & Edwards, R. T. 2007, *A&A*, 469, 607.